Organometallics **2000,** *19,* 1343−1349

Mechanism of *Unlike* Stereoselectivity in 1-Alkene Primary Insertions: Syndiospecific Propene Polymerization by Brookhart-Type Nickel(II) Catalysts

Giuseppe Milano,[†] Gaetano Guerra,*,[†] Claudio Pellecchia,[†] and Luigi Cavallo[‡]

Dipartimento di Chimica, Università di Salerno, 84081 Baronissi (SA), Italy, and
Dipartimento di Chimica, Università di Napoli, 80134 via Mezzocannone 4, Napoli, Italy

Received October 6, 1999

A theoretical QM/MM study of propene polymerization by a Brookhart-type Ni(II) catalyst suggests a mechanism of *unlike* chain end controlled stereoselectivity for 1-alkene primary insertion. The chirality (*si* or *re*) of the tertiary carbon of the growing chain nearest to the metal determines, in the α-agostic-assisted transition state for monomer insertion, the preferential chain orientation around the metal−carbon bond ($\theta_1 \approx -60°$ or $\theta_1 \approx +60°$, respectively). This chiral orientation of the chain, in turn, discriminates by nonbonded repulsive interactions between propene enantiofaces (*re* or *si*, respectively). Analogies and differences with respect to the well-established mechanism of chiral site controlled stereoselectivity for olefin insertion polymerizations are discussed.

1. Introduction

A necessary (but not sufficient) prerequisite for stereospecificity of catalytic systems for alkene polymerization is the stereoselectivity of each monomer insertion step, that is, the ability to discriminate between the two enantiomeric faces of prochiral monomers. This stereoselectivity can be dictated by the chirality of the catalytic site (in most cases the optically inactive catalyst consists of a racemic mixture of enantiomorphic sites) or by the configuration of the asymmetric tertiary C atom of the last inserted monomer unit (generally indicated as *chiral site* and *chain end* stereocontrol, respectively).[1,2] Analysis of distribution of steric defects along the polymer chain, which can be generally obtained by ^{13}C NMR spectra,[1−6] provides insight into the mechanism of steric control. For instance, for mainly syndiotactic propagation, which is considered in the present paper, the presence into *r* dyad sequences of stereodefects consisting prevailingly of isolated and pairs of *m* dyads is expected for chain end and chiral site stereocontrol, respectively (see Scheme 1).

Scheme 1

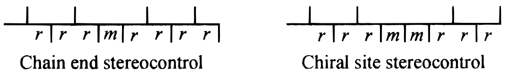

The chiral site stereocontrol can lead to nearly complete stereoselectivity. In fact, it is present in most relevant stereospecific catalytic systems, that is, the isospecific heterogeneous catalysts based on $TiCl_3$ (traditional and supported)[7−9] as well as the isospecific[10,11] and syndiospecific[12] homogeneous catalysts based on chiral metallocene complexes. The high industrial relevance of these processes has brought a large amount of experimental and theoretical studies on the chiral site controlled mechanisms of stereoselectivity (and stereospecificity).

Molecular modeling studies relative to heterogeneous[13−15] as well as homogeneous[16−26] chiral site stereocontrolled catalytic systems have shown that, when a substantial stereoselectivity is calculated for primary propene insertion, this is mainly due to nonbonded interactions of the alkyl substituent of the chirally coordinated alkene monomer with the chirally oriented growing chain. According to this mechanism of *chiral orientation of the growing chain*, the *stereoselectivity* of these models is due to interactions of the π-ligands with the growing chain, determining its chiral orientation, which, in turn, discriminates between the two prochiral faces of the monomer, and not to direct interactions of

---

[†] Università di Salerno.

[‡] Università di Napoli.

(1) Zambelli, A.; Tosi, C. *Adv. Polym. Sci.* **1974**, *31*.

(2) Corradini, P.; Busico, V.; Guerra, G. *Comprehensive Polymer Science*; Allen, G., Bevington, J. C., Eds.; Pergamon Press: Oxford, 1989; Vol. 4, p 29.

(3) Bovey, F. A.; Tiers, G. V. D. *J. Polym. Sci.* **1960**, *44*, 173.

(4) Sheldon, R. A.; Fueno, T.; Tsunetsugu, T.; Furukawa, J. *J. Polym. Sci. Part B* **1965**, *3*, 23.

(5) Doi, Y.; Asakaru, T. *Makromol. Chem.* **1975**, *176*, 507.

(6) Zambelli, A.; Ammendola, P. *Prog. Polym. Sci.* **1991**, *16*.

(7) Natta, G. *Nobel Lectures in Chemistry, 1963−1970*; Elsevier: New York, 1972; p 27.

(8) Ziegler, K. *Nobel Lectures in Chemistry, 1963−1970*; Elsevier: New York, 1972; p 6.

(9) Moore, E. P. J. *Polypropylene Handbook: Polymerization, Characterization, Properties, Applications*; Hanser Publishers: Munich, 1996.

(10) Ewen, J. A. *J. Am. Chem. Soc.* **1984**, *106*, 6355.

(11) Kaminsky, W.; Külper, K.; Brintzinger, H. H.; Wild, F. R. W. P. *Angew. Chem., Int. Ed. Engl.* **1985**, *24*, 507.

(12) Ewen, J. A.; Jones, R. L.; Razavi, A.; Ferrara, J. D. *J. Am. Chem. Soc.* **1988**, *110*, 6255.

(13) Corradini, P.; Barone, V.; Fusco, R.; Guerra, G. *Eur. Polym. J.* **1979**, *15*, 133.

(14) Corradini, P.; Barone, V.; Guerra, G. *Macromolecules* **1982**, *15*, 1242.

(15) Corradini, P.; Barone, V.; Fusco, R.; Guerra, G. *J. Catal.* **1982**, *77*, 32.

(16) Corradini, P.; Guerra, G.; Vacatello, M.; Villani, V. *Gazz. Chim. Ital.* **1988**, *118*, 173.

(17) Cavallo, L.; Corradini, P.; Guerra, G.; Vacatello, M. *Macromolecules* **1991**, *24*, 1784.

(18) Castonguay, L. A.; Rappé, A. K. *J. Am. Chem. Soc.* **1992**, *114*, 5832.

10.1021/om990796e CCC: $19.00
Publication on Web 03/04/2000

the π-ligands with the monomer. The latter can only reinforce or diminish the extent of steric control in certain cases.[26,27] This mechanism of stereoselectivity is in agreement[14] with several experimental data relative to the stereostructures of polymer chain ends[28,29] as well as in agreement[30] with the absolute configurations of products of deuteration and deuteriooligomerizations of 1-alkenes.[31−33] It is worth noting that also fine details of these stereospecific behavior have been rationalized, e.g., the dependence of stereoselectivity and regioselectivity on alkyl substituents of metallocenes,[34] the stereoselectivities relative to occasional secondary monomer insertions or relative to primary insertions following these secondary insertions,[22] and the relationship between regiospecificity and type of stereospecificity.[35]

The chain end stereocontrol leads generally to lower stereoselectivities (differences in activation energy for insertion of the two enantiofaces generally lower than 8 kJ/mol).[1,36,37] For this reason the corresponding catalytic systems have not reached industrial relevance for propene homopolymerization. However, some of them are widely used for propene copolymerization with ethene. Since the 1960s the syndiospecific chain end controlled polymerization of propene in the presence of homogeneous vanadium-based catalytic systems has been known. For these systems, it has been well established that the polymerization is poorly regioselective and that the stereoselective (and possibly syndiospecific) step is propene insertion into the metal secondary carbon bond with formation of a new secondary metal carbon bond.[38−40] Chain end controlled isospecificity and syndiospecificity for 1-alkene polymerizations at low temperatures with achiral metallocenes, occurring through primary monomer insertions, have also been reported in more recent years.[10,36,41−43]

Recently, a syndiospecific chain end controlled propene polymerization by Brookhart-type[44,45] Ni(II) catalysts at low temperatures, also occurring through a primary monomer insertion, has been reported.[46] The polymerization is even less regioselective than in the case of V-based catalysts, but a prevailing primary monomer insertion has been assessed by ^{13}C NMR analysis of suitably labeled polymer end groups formed in both the initiation and termination steps and confirmed by the structure of low molecular weight samples.[46,47] Even more recently, bis(imino)pyridil Fe(II)-based catalysts have been reported to afford isospecific chain end controlled propene polymerization occurring through secondary monomer insertion.[48−50]

Only a few molecular modeling studies relative to the mechanisms of chain end controlled stereoselectivity have been reported. As for V-based catalysts, the reported mechanisms of *unlike* stereoselectivity,[40,51] leading to syndiospecific polymers, require several assumptions not sufficiently supported by the poor knowledge of the nature of the catalytic complexes. A possible mechanism for chain end controlled *like* stereoselectivity, leading to isospecific polymers, was proposed 10 years ago, on the basis of a molecular mechanics (MM) study, for the low-temperature isospecific propene polymerization in the presence of a catalytic system based on unbridged bis(cyclopentadienyl)Ti derivatives.[52]

In the wake of combined quantum mechanics/molecular mechanics (QM/MM) studies on the mechanism of ethene polymerization by the same catalyst,[53] in the present paper we investigate the mechanism of chain end controlled *unlike* stereoselectivity for a Brookhart-type Ni(II) catalyst, whose stereospecific behavior and active catalytic species are well established.[44−47,54] In particular, herein we report a theoretical QM/MM study relative to diastereoisomeric intermediates and transition states corresponding to propene primary insertion for the catalytic system based on diacetyl-bis(2,6-diisopropylphenylimine)nickel derivative (see Scheme 2).

2. Models and Methods

The origin of stereospecificity in a catalytic system is always connected with the energy difference between diastereoisomeric situations, which originate from the combination of two

---

(19) Kawamura-Kuribayashi, H.; Koga, N.; Morokuma, K. *J. Am. Chem. Soc.* **1992**, *114*, 8687.

(20) Hart, J. A.; Rappé, A. K. *J. Am. Chem. Soc.* **1993**, *115*, 6159.

(21) Cavallo, L.; Corradini, P.; Guerra, G.; Vacatello, M. *Polymer* **1991**, *32*, 1329.

(22) Guerra, G.; Cavallo, L.; Moscardi, G.; Vacatello, M.; Corradini, P. *J. Am. Chem. Soc.* **1994**, *116*, 2988.

(23) Pietsch, M. A.; Rappé, A. K. *J. Am. Chem. Soc.* **1996**, *118*, 10908.

(24) Guerra, G.; Cavallo, L.; Moscardi, G.; Vacatello, M.; Corradini, P. *Macromolecules* **1996**, *26*, 4834.

(25) van der Leek, K.; Angermund, K.; Reffke, M.; Kleinschmidt, R.; Goretzki, R.; Fink, G. *Chem. Eur. J.* **1997**, *3*, 58.

(26) Corradini, P.; Cavallo, L.; Guerra, G. In *Metallocene Based Polyolefins, Preparation, Properties and Technology*; Scheirs, J., Kaminsky, W., Eds.; Wiley: Chichester, 2000; Vol. 2, p 3.

(27) Longo, P.; Proto, A.; Grassi, A.; Ammendola, P. *Macromolecules* **1991**, *24*, 4624.

(28) Zambelli, A.; Sacchi, M. C.; Locatelli, P.; Zannoni, G. *Macromolecules* **1982**, *15*, 211.

(29) Longo, P.; Grassi, A.; Pellecchia, C.; Zambelli, A. *Macromolecules* **1987**, *20*, 1015.

(30) Cavallo, L.; Guerra, G.; Corradini, P.; Vacatello, M. *Chirality* **1991**, *3*, 299.

(31) Pino, P.; Cioni, P.; Wei, J. *J. Am. Chem. Soc.* **1987**, *109*, 6189.

(32) Pino, P.; Galimberti, M.; Prada, P.; Consiglio, G. *Makromol. Chem.* **1990**, *191*, 1677.

(33) Gilchrist, J. H.; Bercaw, J. E. *J. Am. Chem. Soc.* **1996**, *118*, 12021.

(34) Toto, M.; Cavallo, L.; Corradini, P.; Guerra, G.; Resconi, L. *Macromolecules* **1998**, *31*, 3431.

(35) Guerra, G.; Cavallo, L.; Corradini, P.; Longo, P.; Resconi, L. *J. Am. Chem. Soc.* **1997**, *119*, 4394.

(36) Resconi, L.; Abis, L.; Franciscono, G. *Macromolecules* **1992**, *25*, 6814.

(37) Erker, G.; Fritze, C. *Angew. Chem., Int. Ed. Engl.* **1992**, *31*, 199.

(38) Zambelli, A.; Tosi, C.; Sacchi, C. *Macromolecules* **1972**, *5*, 649.

(39) Zambelli, A.; Locatelli, P.; Rigamonti, E. *Macromolecules* **1979**, *12*, 156.

(40) Zambelli, A.; Allegra, G. *Macromolecules* **1980**, *13*, 42.

(41) Ewen, J. A. In *Catalytic Polymerization of Olefins*; Keii, T., Soga, K., Eds.; Elsevier: New York, 1986; p 271.

(42) Zambelli, A.; Ammendola, P.; Grassi, A.; Longo, P.; Proto, A. *Macromolecules* **1986**, *19*, 2703.

(43) Ammendola, P.; Pellecchia, C.; Longo, P.; Zambelli, A. *Gazz. Chim. Ital.* **1987**, *117*, 65.

(44) Johnson, L. K.; Killian, C. M.; Brookhart, M. S. *J. Am. Chem. Soc.* **1995**, *117*, 6414.

(45) Killian, C. M.; Templ, D. J.; Johnson, L. K.; Brookhart, M. *J. Am. Chem. Soc.* **1996**, *118*, 11664.

(46) Pellecchia, C.; Zambelli, A.; Oliva, L.; Pappalardo, D. *Macromolecules* **1996**, *29*, 6990.

(47) Pellecchia, C.; Zambelli, A.; Mazzeo, M.; Pappalardo, D. *J. Mol. Catal. A: Chem.* **1998**, *128*, 229.

(48) Small, B. L.; Brookhart, M. *Polym. Prepr.* **1998**, *39*, 213.

(49) Pellecchia, C.; Mazzeo, M.; Pappalardo, D. *Macromol. Rapid Commun.* **1998**, *19*, 651.

(50) Small, B. L.; Brookhart, M. *Macromolecules* **1999**, *32*, 2120.

(51) Guerra, G.; Corradini, P.; Pucciariello, R. *Macromolecules* **1985**, *18*, 2030.

(52) Venditto, V.; Guerra, G.; Corradini, P.; Fusco, R. *Polymer* **1990**, *31*, 530.

(53) Deng, L.; Woo, T. K.; Cavallo, L.; Margl, P. M.; Ziegler, T. *J. Am. Chem. Soc.* **1997**, *119*, 6177.

(54) Pellecchia, C.; Zambelli, A. *Macromol. Rapid Commun.* **1996**, *17*, 333.

Scheme 2

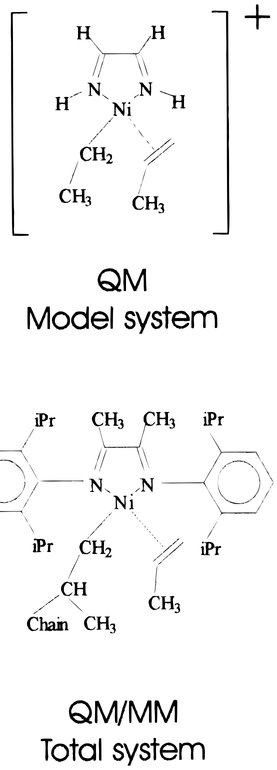

or more of the possible elements of chirality. In this case, the catalytic system presents only two kinds of chirality: (a) chirality of coordination of the prochiral olefin, which can be *si* or *re*;[55] (b) chirality of the nearest tertiary carbon atoms of the growing chain, which can be *R* or *S*.

In particular, the *R* and *S* chiralities can be obtained by a *cis* primary insertion of a *si* and *re* coordinated propene into a growing chain−metal bond, respectively.[56] For these reasons, the growing chains presenting *R* and *S* chirality of the tertiary carbon atom nearest to the metal will be thereafter named *si*- and *re*-ending model chains, respectively. Without loss of generality, our calculations are referenced to a *si*-ending model chain.

The main dihedral angles that are relevant to the present discussion are sketched in Figure 1. In particular, θ_0 is associated with rotation of the olefin around the axis connecting the metal to the center of the double bond, while θ_1, θ_2, θ_3, and θ_4 define the growing chain orientation. $\theta_0 = 0°$ corresponds to the conformation having the Ni−C bond of the growing chain eclipsed with respect to the double bond of the olefin, and $\theta_1 = 0°$ corresponds to the conformation having the first C−C bond of the growing chain eclipsed with respect to the axis connecting the metal atom to the center of the double bond of the olefin. Furthermore near to $\theta_0 = 0°$ the propene is oriented in a way suitable for the primary insertion. The dihedral angles θ_2, θ_3, θ_4 are measured according to the IUPAC rules.[57] As apparent for the model chain of Figure 1, the chirality of the second tertiary carbon atom of the growing chain is not specified (the methylene of the growing chain is modeled by a methyl). As a consequence θ_4 refers to the H atom bound to the tertiary carbon atom, and the dihedral angle will be explicitly indicated as θ_{4H}. Analogously, for the case of the isobutyl groups of structures 2−5 the chirality of the tertiary carbon is not specified, and θ_2 refers to the H atom bound to the tertiary carbon and will be explicitly indicated as θ_{2H}.

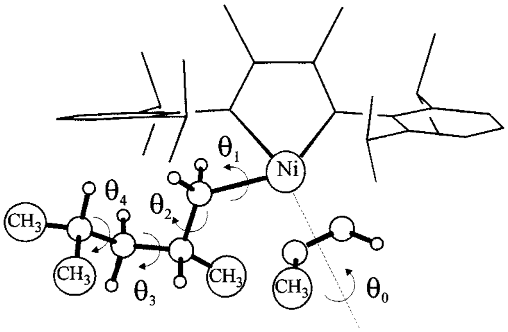

Figure 1. The model catalytic site used in the QM/MM computations. The main dihedral angles that are relevant to the present discussion are sketched. θ_0 is associated with rotation of the olefin around the axis connecting the metal to the center of the double bond, while θ_1, θ_2, θ_3, and θ_4 define the growing chain orientation. Near $\theta_0 = 0°$ the propene is oriented in a way suitable for the primary insertion. $\theta_1 = 0°$ corresponds to the conformation having the first C−C bond of the growing chain eclipsed with respect to the axis connecting the metal atom to the center of the double bond of the olefin.

Computational Details. Stationary points on the potential energy surface were calculated with the Amsterdam Density Functional (ADF) program system,[58] developed by Baerends et al.[59,60] The electronic configurations of the molecular systems were described by a triple-ζ STO basis set on Ni for 3s, 3p, 3d, 4s, and 4p. Double-ζ STO basis sets were used for N and C (2s, 2p) and H (1s). The basis sets on N and C were augmented with a single 3d polarization function except for H, where a 2p function was used. The $1s^22s^22p^6$ configuration on nickel and $1s^2$ configuration on carbon and nitrogen were assigned to the core and treated within the frozen core approximation. Energetics and geometries were evaluated by using the local exchange−correlation potential by Vosko et al.,[61] augmented in a self-consistent manner with Becke's[62] exchange gradient correction and Perdew's[63,64] correlation gradient correction. First-order scalar relativistic corrections were added to the total energy, since a perturbative relativistic approach is sufficient for 3d metals. In view of the fact that all the systems investigated in this work show a large HOMO−LUMO gap, a spin-restricted formalism was used for all calculations.

The ADF program was modified by some of us[53,65,66] to include standard molecular mechanics force fields in such a way that the QM and MM parts are coupled self-consistently, according to the method prescribed by Morokuma and Maseras.[67] The model QM system and the total QM/MM system are reported in Scheme 2. The partitioning of the systems into QM and MM parts involves the skeleton of the catalyst's ligand and the terminal piece of the growing chain; that is, the first two carbon atoms of the growing chain and the monomer are always totally composed by pure QM atoms. Moreover, the five-membered diimine ring, including the metal atom, is also composed by pure QM atoms. The MM atoms, hence, are the methyl groups on the diimine ring, the 2,6-diisopropylphenyl groups of the ligand, and the carbons and hydrogen atoms needed to transform the pure QM ethylic growing chain into

---

(55) Hanson, K. R. *J. Am. Chem. Soc.* **1966**, *88*, 2731.

(56) Corradini, P.; Guerra, G.; Barone, V. *Eur. Polym. J.* **1984**, *20*, 1177.

(57) IUPAC Commission of Macromolecular Nomenclature. *Pure Appl. Chem.* **1979**, *51*, 1101.

(58) *ADF 2.3.0 Users Guide*; Vrije Universiteit Amsterdam: Amsterdam, The Netherlands, 1996.

(59) Baerends, E. J.; Ellis, D. E.; Ros, P. *Chem. Phys.* **1973**, *2*, 41.

(60) te Velde, B.; Baerends, E. J. *J. Comput. Phys.* **1992**, *99*, 84.

(61) Vosko, S. H.; Wilk, L.; Nusair, M. *Can. J. Phys.* **1980**, *58*, 1200.

(62) Becke, A. *Phys. Rev. A* **1988**, *38*, 3098.

(63) Perdew, J. P. *Phys. Rev. B* **1986**, *33*, 8822.

(64) Perdew, J. P. *Phys. Rev. B* **1986**, *34*, 7406.

(65) Cavallo, L.; Woo, T. K.; Ziegler, T. *Can. J. Chem.* **1998**.

(66) Woo, T. K.; Cavallo, L.; Ziegler, T. *Theor. Chem. Acc.* **1998**, *100*, 307.

(67) Maseras, F.; Morokuma, K. *J. Comput. Chem.* **1995**, *16*, 1170.

the longer isobutyilic or 2,4-dimethylpentanylic groups, used to model an achiral and a chiral growing chain, respectively. H atoms have been used as capping atoms.[53]

In the optimization of the MM part, the difference between the C−H (growing chain), C−H (diimine ring), and N−H bonds crossing the QM/MM border, and the corresponding optimized C−C (growing chain), C−C (between the carbons of the diimine ring and their methylic substituents), and N−C distances, were fixed equal to 0.43, 0.40, and 0.36 Å, respectively. This corresponds to optimized C−C (growing chain), C−C (between the carbons of the diimine ring and their methylic substituents), and N−C distances roughly equal to 1.54, 1.50, and 1.40 Å, respectively. This coupling scheme is described in detail in ref 67.

The Karplus molecular mechanics CHARMM force field,[68] as extended by Bosnich for bent metallocenes,[69] has been adopted. The Ni atom was assigned the Ni4+2 van deer Waals parameters of Rappé's UFF.[70] Electrostatic interactions were not included in the molecular mechanics potential. Further details on the methodology can be found in previous papers.[53,65−67,71]

All the structures that will follow are stationary points on the combined QM/MM potential surface. Geometry optimizations were terminated if the largest component of the Cartesian gradient was smaller than 0.002 au. Transition state geometries were approached by a linear-transit procedure, using the distance between the C(olefin) and C(chain) atoms which are going to form the new C−C bond as reaction coordinate, while optimizing all other degrees of freedom. Full transition state searches were started from geometries corresponding to maxima along the linear-transit curves. At the end of each transition state search, the approximated Hessian presented one negative eigenvalue. No symmetry constraints were used. The accuracy of the DFT approach utilized here has recently been verified in a very similar Pd(II) system, where the barrier heights were found to be within 12−20 kJ/mol of experimental measurements.[72,73]

3. Results and Discussion

Metal−Alkyl and Olefin Coordination Complexes. As a preliminary step for the definition of coordination intermediates and transitions states for primary propene insertion into the Ni−C(chain) σ-bond, the achiral isobutyl alkyl group has been assumed as a growing chain. The optimized geometry of the Ni complex with the isobutyl group β-agostic coordinated to the metal, and monomer-free (structure **1**), is very similar to the β-agostic resting state **1a** found by Ziegler and co-workers for ethene polymerization with the same catalyst.[53] Also in the present case, the Ni, C_α, C_β, and β-H atoms are coplanar ($\theta_{2H} = 0$) and lie on the Ni diimine ring plane.

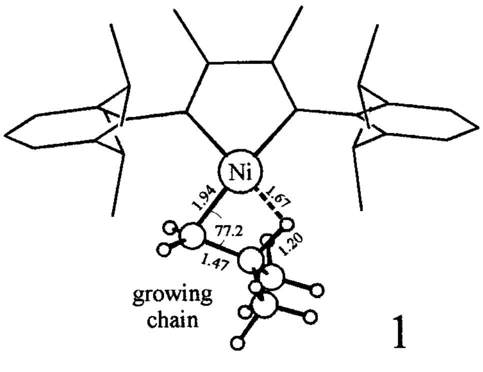

1

Structure **2** is the optimized geometry of a possible coordination intermediate involving a *re*-coordinated propene. The monomer coordination pushes the C_β atom of the growing chain out of the diimine ring plane (θ_1 close to −120°). Although θ_{2H} remains close to 0°, the longer Ni−H(agostic) distance suggests a weaker β-agostic interaction. The Ni−H(agostic) distance is also considerably longer than the analogous distance (1.88 Å) in the corresponding coordination intermediate **2a** for the ethene polymerization with the same catalyst.[53] The double bond of the olefin is nearly perpendicular to the Ni−C_α bond ($\theta_0 = -88°$). Moreover, the Ni−CH_2(propene) distance, 2.09 Å, is close to Ni−CH_2(ethene) distances (2.08 Å),[53] while the Ni− CH(propene) distance is slightly longer (2.20 Å). A nearly isoenergetic minimum (energy difference of 2 kJ/mol) occurs for $\theta_1 \approx +120°$, $\theta_0 \approx +88°$, maintaining $\theta_{2H} \approx 0°$.

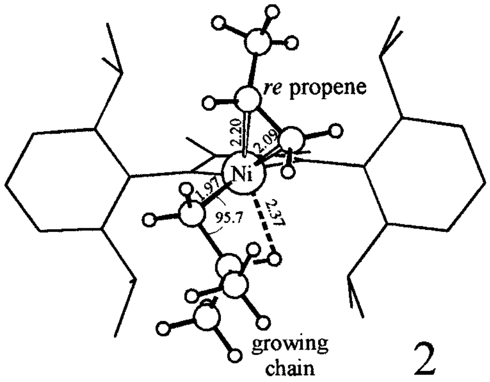

2

For these complexes, propene coordination energies of nearly 37 kJ/mol have been calculated. This coordination energy gain is lower than those calculated for ethene (≈54 kJ/mol)[53] and would be of the same order of magnitude of the association entropy loss.[74−76] Hence, this coordination intermediate possibly does not represent the resting state.[84]

Transition States for Olefin Insertion into the Isobutyl Group. Three possible transition states corresponding to primary insertion of *re* propene have been found, and their geometry is reported in structures **3a**, **3b**, and **3c**. As usual for alkene polymerization reactions, the hydrogen β-agostic interaction is replaced by a α-agostic one during the insertion process.[77−80] It has to be noted that the formation of the α-agostic interaction brings the second carbon of the growing chain out

---

[68] Brooks, B. R.; Bruccoleri, R. E.; Olafson, B. D.; States, D. J.; Swaminathan, S.; Karplus, M. *J. Comput. Chem.* **1983**, *4*, 187.

[69] Doman, T. N.; Hollis, T. K.; Bosnicj, B. *J. Am. Chem. Soc.* **1995**, *117*, 1352.

[70] Rappé, A. K.; Casewit, C. J.; Colwell, K. S.; Goddard, W. A., III; Shiff, W. M. *J. Am. Chem. Soc.* **1992**, *114*, 10024.

[71] Margl, P. M.; Woo, T. K.; Ziegler, T. *Organometallics* **1998**, *17*, 4997.

[72] Margl, P. M.; Ziegler, T. *Organometallics* **1996**, *15*, 5519.

[73] Margl, P. M.; Ziegler, T. *J. Am. Chem. Soc.* **1996**, *118*, 7337.

[74] Rix, F. C.; Brookhart, M.; White, P. S. *J. Am. Chem. Soc.* **1996**, *118*, 4746−4764.

[75] Musaev, D. G.; Froese, R. D. J.; Svensson, M.; Morokuma, K. *J. Am. Chem. Soc.* **1997**, *119*, 367.

[76] Margl, P. M.; Deng, L.; Ziegler, T. *Organometallics* **1998**, *17*, 933.

[77] Brookhart, M.; Green, M. L. H.; Wong, L. *Prog. Inorg. Chem.* **1988**, *36*, 1.

[78] Piers, W. E.; Bercaw, J. E. *J. Am. Chem. Soc.* **1990**, *112*, 9406.

[79] Kraudelat, H.; Brintzinger, H. H. *Angew. Chem., Int. Ed. Engl.* **1990**, *29*, 1412.

[80] Lohrenz, J. C. W.; Woo, T. K.; Ziegler, T. *J. Am. Chem. Soc.* **1995**, *117*, 12793.

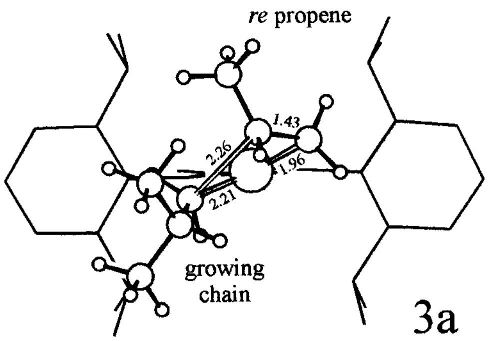

3a

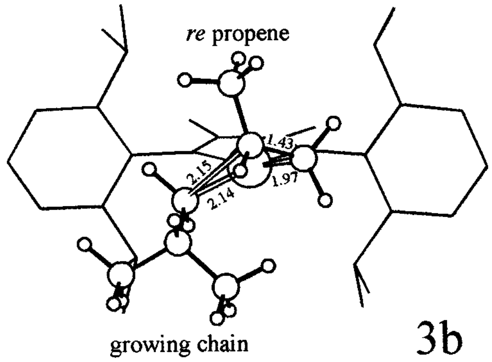

3b

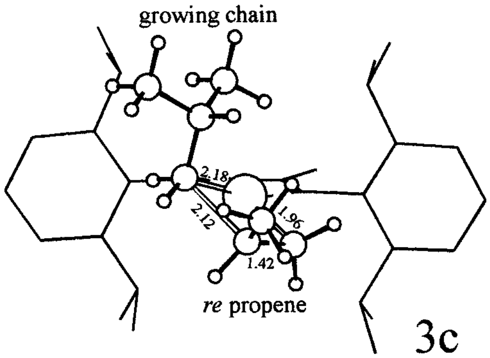

3c

of the plane defined by the metal and by the monomer double bond ($\theta_1 \approx -56°$, $-68°$ and $+104°$ in **3a**, **3b**, and **3c**, respectively). As usual for this class of reactions, the four-center transition state is almost coplanar. This generally corresponds to values of θ_0 close to 0°. However, the combined bulkiness of the diimine ligand, propene, and isobutylic growing chain deforms the transition state from its "ideal" planar geometry and can lead to values of $|\theta_0|$ up to 35°. This feature is retained also in the transition states of the next section.

The transition states **3a** and **3b** present negative values of θ_1 for the *re* propene insertion, and the main difference is the value assumed by θ_{2H}. Transition state **3a** has a θ_{2H} value close to 0°, as in the coordination intermediate **2**, whereas transition state **3b** has a θ_{2H} value close to 100° and is more stable than **3a** by 6 kJ/mol. The energy difference is essentially due to larger nonbonded repulsive interactions associated with the shortest distance between a growing chain methyl group and a propene carbon atom for $\theta_{2H} \approx 0°$ (3.14 Å in structure **3a**) than for $\theta_{2H} \approx 100°$ (3.35 Å in structure **3b**). Furthermore, the calculated energy difference between the β-agostic coordination intermediate **2** and the most stable transition state **3b** is 41 kJ/mol.

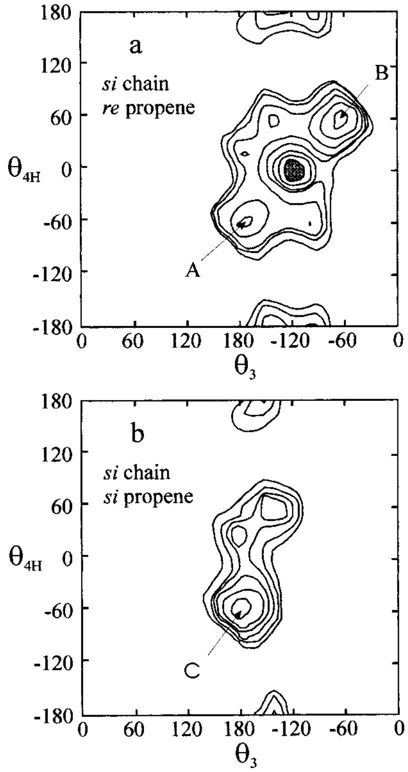

Figure 2. Conformational MM energy maps $E(\vartheta_3, \vartheta_{4H})$ relative to *re* and *si* propene insertion into a *si*-ending chain. For the for *re* and *si* propene, values of $\theta_0 \approx 35°$, $\theta_1 \approx -68°$, and $\theta_{2H} \approx 100°$ and values of $\theta_0 \approx -35°$, $\theta_1 \approx 68°$, and $\theta_{2H} \approx -100°$ have been used, respectively. In part a, the letters A and B indicate the conformational minima of the growing chain corresponding to transition state structures **4a** and **4b**, respectively. In part b, the letter C indicates the conformational minimum of the growing chain corresponding to the transition state structure **4c**. The isoenergetic curves are spaced by 4 kJ/mol.

Transition state **3c**, instead, is characterized by a positive values of θ_1 for the *re* propene insertion, and it presents the second carbon atom of the growing chain and the *re* propene methyl group on the same side of the plane defined by the metal and by the monomer double bond. Transition state **3c** is higher in energy, 17 kJ/mol above transition state **3b**. Transition states presenting the C_β atom of the growing chain and the propene methyl group on the same side of the above-defined plane have been calculated to be of higher energy also for models of stereospecific heterogeneous and homogeneous polymerization catalysts.[26,34]

Before concluding this section, we want to remark that in the presence of the achiral growing chain (isobutyl group), strictly analogous results would have been obtained by considering the coordination and insertion of a *si* propene molecule. To obtain the *si* propene geometries, only a change of sign of the diedhral angles of the corresponding *re* geometries is required. For example, to the most stable transition state **3b** for *re* propene insertion, with $\theta_0 \approx 35°$, $\theta_1 \approx -68°$, and $\theta_{2H} \approx 100°$, an isoenergetic transition state for *si* propene insertion, with $\theta_0 \approx -35°$, $\theta_1 \approx 68°$, and $\theta_{2H} \approx -100°$, corresponds.

Transition States for Olefin Insertion into a Chiral Growing Chain. To find accessible conformations for the chiral growing chain, here modeled by the 2,4-dimethylpentanyil group, we performed preliminary MM calculations by fixing the geometrical parameters of the QM domain to the values obtained for the transition states **3a** and **3b**. For the most stable transition state **3b**, the conformational MM energy maps $E(\vartheta_3, \vartheta_{4H})$ relative to *re* and *si* propene insertion into a *si*-ending chain (corresponding to an *R* chirality of the 2,4-dimethylpentanyil group) are shown in Figure 2a and 2b, respectively.

The map of Figure 2a, relative to a *si*-ending chain when a propene is *re* coordinated, is nearly typical of an unconstrained polypropene chain (see, for example, Figure 3 in ref 56 and ref 81). In fact, as for the dihedral ϑ_3 corresponding to a bond presenting a negative configurational sign,[82] similar energy minima for T and G^- conformations are obtained. Starting from the structures corresponding to the conformations labeled A and B in the MM energy map of Figure 2a, full QM/MM transition state search led to structures **4a** and **4b**, labeled syndio-T and syndio-G, respectively. It is clear that in both structures the chain grows in a free sector, and repulsive interactions of the successive chain atoms with the other metal ligands are avoided.

On the other hand, the map of Figure 2b relative to a *si*-ending chain when a propene is *si* coordinated shows the presence of some constraints on the polypropene chain conformation. In fact, conformations with the dihedral angle $\vartheta_3 \approx -60°$ are strongly destabilized by repulsive interactions between the growing chain and the propene molecule, whereas the minimum energy conformation with $\vartheta_3 \approx 180°$ (labeled C) is almost isoenergetic with minima labeled A and B (the largest energy difference is 1 kJ/mol). Starting from structure C, full QM/MM transition state search led to structure **4c**, labeled iso-T. Also in this case, the growing chain develops in a free sector, and repulsive interactions with the metal ligands are avoided.

Finally, the preference for transition states presenting $|\theta_{2H}| \approx 100°$, previously discussed for an isobutylic growing chain, is confirmed and enhanced for the longer and chiral 2,4-dimethylpentanyil growing chain. In fact, the calculated QM/MM transition states presenting $\theta_{2H} \approx 0°$ are higher in energy by at least 10 kJ/mol relative to transition states presenting $|\theta_{2H}| \approx 100°$, when the larger and chiral growing chain is considered.

In conclusion, three energetically nearly equivalent transition states, **4a**, **4b**, and **4c**, have been located for propene insertion into a *si*-ending growing chain. Two of them, **4a** and **4b**, correspond to *re* propene insertion, while the remaining, **4c**, corresponds to *si* propene insertion. Hence, the present mechanism implies an entropy-driven 2:1 preference for *unlike* enchainment. The small energy differences calculated for the three possible transition states give an overall preference for the *unlike* enchainment at −78 °C close to 3:1. This stereoselectivity would correspond to a fraction of *r* dyads in the polymer chain equal to 0.75.

Replacement of the isopropyl substituents as well as of the methyl subtituents of the diacetylbis(phenylimine) ligand by smaller as well as bulkier substituents does not change significantly the structrure of the transition states and the calculated stereoselectivity of the insertion reactions. These results are in fair agreement with the low stereoselectivities observed for all the catalysts of this class, for which % *r* dyads is in the range 0.52−0.86.[54,83]

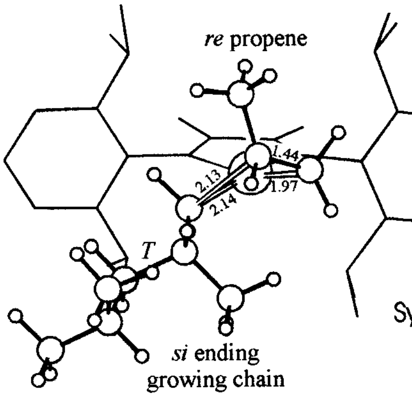

Syndio T

4a

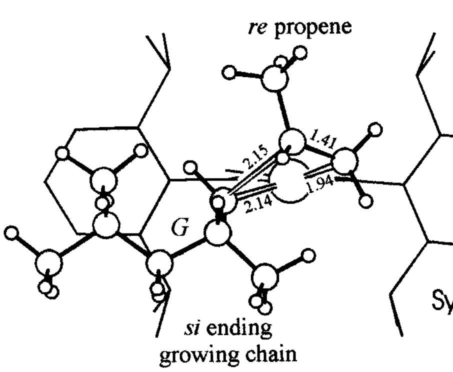

Syndio G

4b

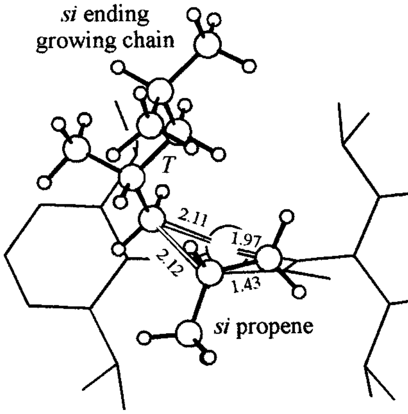

Iso T

4c

4. Conclusions

For the considered catalytic complex, *si*- and *re*-ending chains present higher conformational freedom in transition states for *re* and *si* propene insertions, respectively. Specifically, for the *like* insertion there is only one transition state for $|\theta_1| \approx 68°$, $|\theta_{2H}| \approx 100°$, and $\theta_3 \approx 180°$, while for the *unlike* insertion there is, besides that

---

(81) Suter, U. V.; Flory, P. J. *Macromolecules* **1975**, *8*, 765.

(82) Corradini, P. In *The Stereochemistry of Macromolecules*; Ketley, A. D., Ed.; Marcel Dekker: New York, 1968; Vol. 3, Chapter 1, p 1.

(83) Pellecchia, C. Unpublished results.

(84) Note Added in Proof: The absence of an olefin coordination complex has been recently confirmed by NMR studies: Svejda, S. A.; Johnson, L. R.; Brookhart, M. *J. Am. Chem. Soc.* **1999**, *121*, 10634.

one, an energetically nearly equivalent transition state for $|\theta_1| \approx 68°$, $|\theta_{2H}| \approx 100°$, and $|\theta_3| \approx 60°$. It is worth noting that this mechanism for chain end control of syndiotacticity (i.e., *unlike* stereoselectivity) is critically dependent on the growing chain conformation and in particular on the θ_2 value. For instance, the distances from the metal center of the two carbon atoms of the chain being in position γ with respect to the metal are largely different for $|\theta_{2H}|$ 100° (≈3.8 Å, ≈4.5 Å, see structure **3b**), while they are nearly identical for $\theta_{2H} \approx 0°$ (≈4.5 Å, see structure **3a**).

It is also worth noting that the present mechanism of chain end controlled stereoselectivity presents relevant analogies with the well-established mechanism of chiral site controlled stereoselectivity. In fact, for both mechanisms, the selection between the two monomer prochiral faces is operated by the chiral orientation of the growing chain. In particular, the preferred insertion of a *re* or a *si* propene enantioface is essentially determined by the internal rotation angle relative to the metal–carbon bond θ_1, which, for transition states involving the formation of an α-hydrogen agostic bond, assumes values close to $+60°$ or $-60°$, respectively.

This chiral orientation of the growing chain can be strictly imposed by the chirality of the site. According to our calculations, in the absence of chirality of the site, a chiral orientation of the growing chain can be determined by the chain end chirality. In particular, for the considered catalytic complex, *si*- and *re*-ending chains have higher conformational freedom in transition states presenting $\theta_1 \approx +60°$ and $\theta_1 \approx -60°$, respectively. This, in turn, determines the preference for *re* and *si* monomer insertion and hence the *unlike* stereoselectivity (and syndiospecificity) of the catalytic system. This conclusion is analogous to that of the less rigorous MM study relative to the catalytic system based on unbridged bis(cyclopentadienyl)Ti derivatives.[52] In fact, in that case for *si*- and *re*-ending chains the propene insertion path would be easier for $\theta_1 \approx -60°$ and $+60°$, determining the preference for *si* and *re* monomer insertion and hence the *like* stereoselectivity (and isospecificity) of the catalytic system.

On this basis, we suggest that the mechanisms of chain end controlled stereoselectivity both like and unlike, at least for primary propene insertion, could be considered as a subcase of the more general mechanism of the *chiral orientation of the growing chain*.

Acknowledgment. We thank Prof. P. Corradini, of the University of Naples, and Prof. A. Zambelli, of the University of Salerno, for useful discussions. The financial support of the "Ministero della Ricerca Scientifica e Tecnologica" of Italy (PRIN98) and of Montell Polyolefins is gratefully acknowledged.

OM990796E